PHYSICAL REVIEW A VOLUME 25, NUMBER 1 JANUARY 1982

Photofragment spectroscopy of CH^+: Laser excitation of shape resonances in the $A\ ^1\Pi$ state

H. Helm and P. C. Cosby
Molecular Physics Laboratory, SRI International, Menlo Park, California 94025

M. M. Graff and J. T. Moseley
Department of Physics, University of Oregon, Eugene, Oregon 97403

(Received 14 August 1981)

Rotationally quasibound levels (shape resonances) in the $A\ ^1\Pi$ state of CH^+ are investigated with the use of a coaxial fast-ion-beam—laser photofragment spectrometer. Individual shape-resonance levels are excited with laser radiation from high rotational levels of the $X\ ^1\Sigma^+$ ground state of CH^+. The dissociative decay of the quasibound levels into $C^+(^2P)+H(^2S)$ is monitored by observation of the charged photofragment and measurement of its kinetic energy. Analysis of the excitation wavelength spectrum, the photofragment kinetic energies, and in some cases, the width of the shape resonances allows the assignment of the quantum numbers which characterize the quasibound levels. An improved potential-energy curve for the $A\ ^1\Pi$ state is determined by the comparison of the experimental levels with those calculated for trial potentials. Thirty-two quasibound levels have been identified experimentally as grouping into Λ-doublet components for rotational quantum numbers $12 \leq J' \leq 35$ and vibrational quantum numbers $0 \leq v' \leq 10$. Spectroscopic constants for the $X\ ^1\Sigma^+$ and $A\ ^1\Pi$ states are obtained from a correlated fit of the excitation spectra for the shape-resonance levels and previous spectroscopic observations of the bound levels. Our study also allowed the first direct experimental determination of the dissociation energy of CH^+: $D_0^0 = 4.080 \pm 0.003$ eV.

I. INTRODUCTION

The suspected importance of the radiative recombination reaction

$$C^+(^2P_{1/2})+H(^2S) \rightarrow CH^+(A\ ^1\Pi)\ , \tag{1.1a}$$

followed by

$$CH^+(A\ ^1\Pi) \rightarrow CH^+(X\ ^1\Sigma^+)+h\nu \tag{1.1b}$$

in the interstellar medium has prompted numerous theoretical attempts to calculate the recombination rate coefficient.[1–5] It is generally agreed that this coefficient is small ($\simeq 10^{-17}$ cm^3 s^{-1}) so that direct experimental measurement cannot be used to check the soundness of the various theoretical approaches. The dynamical calculations require detailed knowledge of the potential-energy curves, the transition moment between the A and X states, and the spin-orbit and rotational coupling among the molecular eigenstates of CH^+. These calculations have had to rely almost exclusively on *ab initio* calculations[6] of these properties. The importance of the first two, the potential-energy curves and the transition moment, is obvious. Spin-orbit and rotational coupling effects play an important role in reaction (1.1), since the $A\ ^1\Pi$ state, which allows the radiative stabilization, does not correlate adiabatically with the $C^+(^2P_{1/2})+H(^2S)$ dissociation limit.[4] This may be seen from Fig. 1 where we show schematically the lowest-potential-energy curves of CH^+ with greatly exaggerated spin-orbit splitting at large internuclear distance. Collisions between C^+ and H are rather infrequent in the low-density environment of interstellar space, so that the lifetime[7] for radiative deexcitation

$$C^+(^2P_{3/2}) \rightarrow C^+(^2P_{1/2})+h\nu\ , \tag{1.2}$$

which is ~ 30 s, is short enough that nearly all encounters leading to the radiative recombination event originate from $C^+(^2P_{1/2})+H(^2S)$. The radiative association reaction must therefore involve a nonadiabatic transition from the lowest dissociation limit into the $A\ ^1\Pi$ state.

Nonadiabatic transitions between the singlet and

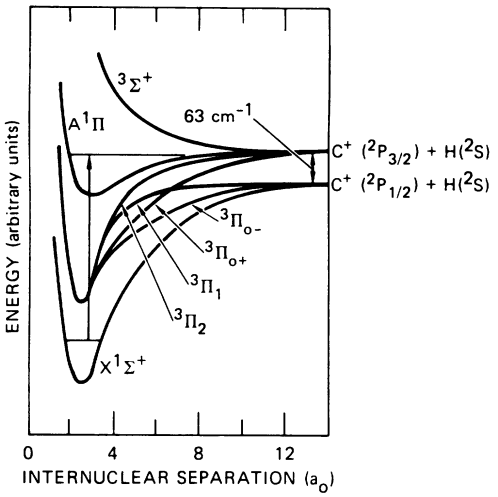

FIG. 1. Schematic of the lowest-potential-energy curves of CH^+. The spin-orbit splitting, as given in Ref. 4, is greatly exaggerated.

triplet manifolds are also of crucial importance in the fine-structure changing reaction

$$C^+(^2P_{1/2})+H(^2S)\rightarrow C^+(^2P_{3/2}) +H(^2S)-63.4\ \text{cm}^{-1}\ , \tag{1.3}$$

which, followed by the radiative deexcitation (1.2), is regarded to provide an important cooling mechanism in diffuse interstellar clouds.[8] Extensive theoretical calculations[9,10] on the partial wave and total cross sections for reaction (1.3) have been carried out at energies between 10 and 100 meV.

The profound importance of CH^+ as a basic building block of larger molecules in interstellar space warrants an experimental study which is capable of providing a critical evaluation of the theoretical calculations on reactions (1.1) and (1.3). We show here that experimental studies of dynamic details of reactions (1.1) and (1.3) are indeed possible using photofragment-spectroscopic techniques, through the observation of shape resonances in the $A\ ^1\Pi$ state. At energies below $\sim$200 meV these resonances influence the cross sections for reactions (1.1) and (1.3) in a decisive manner.[5,10] Using a laser these resonances are selectively excited from individual rotational levels in the $CH^+\ X\ ^1\Sigma^+$ state. Analysis of these exciting transitions has provided the energies of high rotational levels for the A and X states and the dissociation energy of CH^+.

II. SHAPE RESONANCES

The addition of the centrifugal energy term

$$V_{\text{rot}}(R)=[J(J+1)-\Omega^2]\hbar^2/2\mu R^2 \tag{2.1}$$

to the rotationless potential-energy curve of a bound state, such as shown in Fig. 2, produces an effective potential-energy curve with a rotational barrier at large internuclear distances (shown for $J=32$). For a selected range of rotational quantum numbers J, quasibound vibrational levels which lie above the dissociation limit will appear in the well of the effective potential curve. These levels are termed shape resonances. In the absence of other nearby electronic states, these levels predissociate by barrier penetration, the predissociation lifetime being determined by the shape of the effective potential-energy curve and the reduced mass of the quasibound system.

Quantum-mechanical calculations of the shape resonances supported by the $CH^+\ A\ ^1\Pi$ state have been carried out by Abgrall, Guisti-Suzor, and Roueff,[5] Uzer and Dalgarno,[11] and Graff and Moseley.[12] The first two calculations were based on *ab initio* potential-energy curves for the A state. The latter constructed an empirical potential by combining the calculated long-range interaction potential given by Launay and Roueff[9] with a Rydberg-Klein-Rees (RKR) potential, adjusted to fit the currently accepted value for the dissociation energy of the $CH^+\ X\ ^1\Sigma^+$ state.[13] In Fig. 3(a) we show the calculated resonances predicted by Uzer and Dalgarno.[11] The widths of the resonances

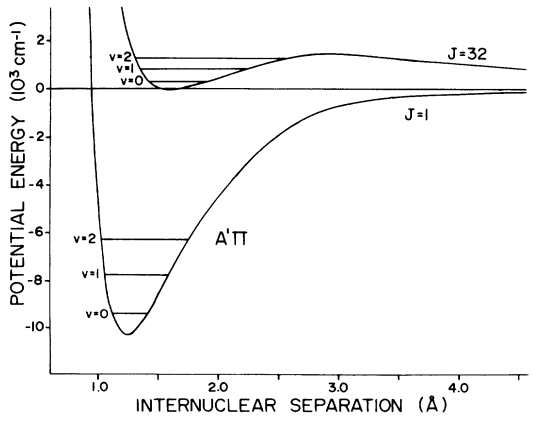

FIG. 2. Rotationless potential-energy curve for the $A\ ^1\Pi$ state of CH^+ ($J=1$) and shape-resonance levels of $v=0$, 1, and 2 supported by this potential for $J=32$.

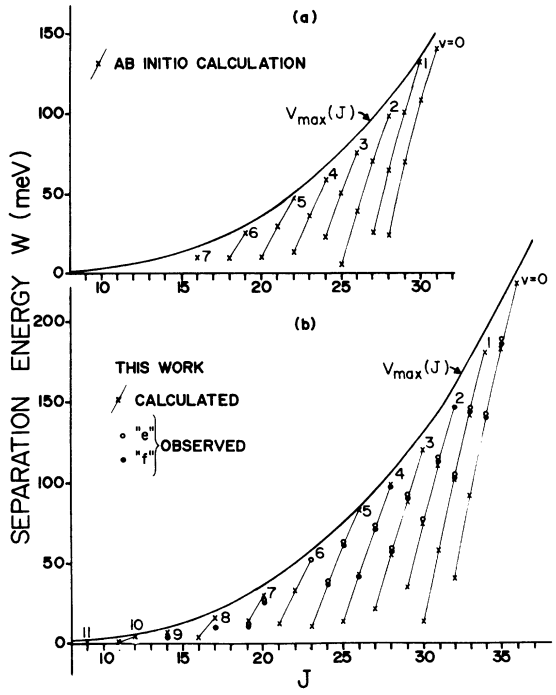

FIG. 3. (a) Shape-resonance levels supported by the $A\ ^1\Pi$ state of CH^+ from the *ab initio* calculations of Ref. 11. (b) Shape-resonance levels observed in the present study are shown by the full and open circles. Levels calculated with the potential given in Table III are shown by the crosses. $V_{max}(J)$ denotes the limiting curves of dissociation.

shown in Fig. 3(a) vary over 36 orders of magnitude. For a given value of v', the vibrational quantum number in the A state, the resonances with the highest rotational quantum numbers (J'), correspond to levels near the top of the rotational barrier. These levels exhibit the largest widths, calculated to be $\gtrsim 1\ cm^{-1}$ which corresponds to predissociation lifetimes $\lesssim 5$ ps.

In low-energy collisions shape resonances manifest themselves through resonant enhancement[14] of the partial-wave cross section σ_l for $J=l$ in the vicinity of the resonance energy E_l. The effects of shape resonances in ion-atom interactions have not yet been observed in scattering experiments, since the maximum energy for shape resonances is typically only a few hundred meV for well depths of the rotationless energy curve of a few eV. Ion-transport coefficients obtained in swarm experiments, while extremely sensitive to transport cross sections at low energies, provide no information about the details of shape resonances, since their effects are integrated over a broad energy distribution.[15] Shape resonances have long been studied in ordinary absorption spectra of diatomic molecules.[16] Transitions are observed from vibrational levels in the ground electronic state of a stable diatomic molecule to quasibound levels in an excited electronic state, the transitions being lifetime broadened by the rotational predissociation of the quasibound level. In all of these studies the energy of quasibound levels with respect to the dissociation limit must be inferred indirectly from the variation of the linewidth with rotational quantum number for various isotopes. In addition, direct photoabsorption measurements are not generally applicable to ionic systems due to the difficulty of preparing adequate concentrations of the absorbing species.

Direct systematic studies of shape resonances in ion-atom systems have become possible with the advent of translational spectroscopy.[17] In these experiments, high-resolution momentum analysis of fragments from unimolecular decay of shape resonances has allowed the determination of the energies and widths of the quasibound levels for the systems H_2^+, HeH^+, and He_2^+, and their isotopic combinations.[17–21] In these studies population of the resonances is generally accomplished by collisional excitation. Since this excitation is not selective, the finite resolution of the momentum analysis makes unambiguous assignment of the quantum numbers difficult in systems with many close-lying resonances. In addition, the technique provides little information on the widths of the resonances.

We show here that selective excitation of shape resonances with a laser is experimentally feasible. When combined with the analysis of the fragment separation energy which is released in the dissociative decay of the shape resonances, this approach allows direct determination of the energies of the resonance levels with respect to the dissociation limit, the determiniation of their widths, and the resolution of fine-structure effects. This technique provides detailed information on low-energy ion-atom collisions dynamics and is readily applicable to many ion-atom systems.

III. EXPERIMENTAL

The experiments were performed in the SRI laser-coaxial ion-beams spectrometer which has been described in detail previously.[22] CH^+ ions

are produced by dissociative ionization of C_2H_2 or CH_4 in an electron-impact (60—200 eV) ion source, accelerated to typically 4000 eV, mass selected, and collimated into a beam with an angular divergence of 2 mrad. An electrostatic quadrupole field allows the ion beam to merge with a laser beam over a distance of 50 cm. In this region discrete states of the CH^+ ion which are coupled to the continuum can be selectively excited from individual rovibronic levels of CH^+ present in the beam and observed through the resulting dissociation. The C^+ fragment ions produced in the laser interaction region are energy selected by an electrostatic analyzer and detected by an electron multiplier. When single-frequency laser radiation is used a resolution of ~ 100 MHz is achieved in the excitation process due to the narrow Doppler breadth in the ion beam. Multimode dye lasers were employed for most of the current work, however, limiting the resolution to approximately 1 cm^{-1}.

As will be discussed in subsequent sections of this paper, we are able to pump electronic transitions into quasibound levels of the $CH^+ A\ ^1\Pi$ state from rotational levels $J'' \leq 36$ and vibrational levels $v'' \leq 5$ of the ion's $X\ ^1\Sigma^+$ ground state. Thus, as much as 1.8 eV of rotational excitation and an equivalent amount of vibrational energy is present in the CH^+ ion beam. From the observed photofragment signals, we estimate a fractional population of $\sim 10^{-7}$ for the higher rotational levels in the beam. We further find that CH^+ is produced with comparable degrees of internal excitation when formed from dissociative ionization of either acetylene or methane. The recent laser-induced fluorescence studies of Grieman, Mahan, O'Keefe, and Winn[23] have found a rotational temperature of 3000 K for CH^+ produced from these molecules. Both studies employed electron energies well above the appearance potential of CH^+. Hence, radiative relaxation of highly excited CH^+ electronic states, which are known from metastable-decomposition studies[24] to be populated by the dissociative ionization of C_2H_2, may be responsible for the high degree of vibrational excitation present in the ion.

IV. OBSERVED SPECTRA

In a previous publication,[25] Cosby, Helm, and Moseley have reported the observation of laser-induced predissociation of CH^+ as a function of excitation wavelength near 3500 Å. Over a narrow wavelength range, 37 transitions were observed to populate discrete states, which predissociate into $C^+ + H$ with separation energies within 350 cm^{-1} above the dissociation limit. (The separation energy, denoted hereafter as W, is the total kinetic energy gained by the dissociating fragments in the center-of-mass frame.) The density and energies of these predissociated levels was clearly incompatible with the predictions for shape resonances in the $CH^+ A\ ^1\Pi$ state and excitation of these levels from the ground state $X\ ^1\Sigma^+$ alone. Alternative explanations for these transitions have been proposed.[25]

In the present investigation the wavelength dependence for the production of C^+ photofragments was measured at photon energies ranging from 16 000 to 19 600 cm^{-1} at low (1 cm^{-1}) resolution using coumarin 540, coumarin 7, sodium fluorescein, and rhodamine 6G dyes. Doppler tuning of the ion beam was used to cover limited wavelength ranges (~ 5 cm^{-1}) in the vicinity of various discrete lines of single-frequency argon-ion and krypton-ion lasers. Several hundred transitions were observed leading to the fragmentation of CH^+ into $C^+ + H$. They, together with those reported earlier,[25] may be classified into three groups: (a) bandlike structures extending over > 1000 cm^{-1} leading predominantly to photofragments with separation energies of less than 25 meV, (b) isolated transitions, scattered over the entire observed wavelength range, producing photofragments with separation energies $\lesssim 200$ meV, and (c) isolated transitions in the uv excitation range (only) which produce photofragments with separation energies between $\sim 1-2$ eV.

In this paper only the transitions of group (b) are discussed in detail. These transitions are conclusively identified as transitions from the $X\ ^1\Sigma^+$ state to shape resonances in the $A\ ^1\Pi$ state.

A typical wavelength spectrum for the production of photofragments of groups (a) and (b) (with energies between 0 and ~ 200 meV) is shown in Fig. 4. For this spectrum the experiment was operated within the dye-laser cavity. The interaction of ions with the laser light propagating parallel and antiparallel to the ion beam leads to a characteristic doubling of all transitions into two Doppler components. At a parent-ion energy of 2700 eV the two components are separated by ~ 24 cm^{-1} at a photon energy of 18 000 cm^{-1}. These respective Doppler components are marked in Fig. 4 for transitions which were later identified as exciting shape-resonance levels of the A state. For this spectrum the energy analyzer was set to accept

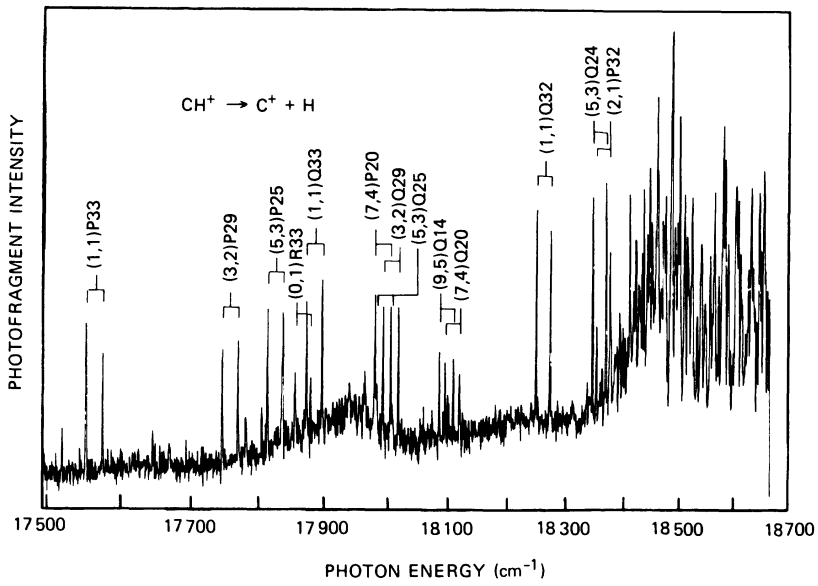

FIG. 4. Low-resolution (1 cm^{-1}) dye-laser scan showing the production of photofragments with kinetic energies in the range between 0 and $\sim$200 meV. The CH^+ ions were irradiated in the laser cavity; hence each transition appears as a Doppler doublet. Doppler doublets identified as transitions to shape-resonance levels are marked by the quantum numbers $(v',v'')\Delta JJ''$.

all photofragments which fall within the solid angle of the aperture to the energy analyzer. A bandlike feature appears in Fig. 4 near 18 350 cm^{-1} which extends to above 19 600 cm^{-1} with comparable intensity. Wavelength scans covering a fraction of this feature are shown in Fig. 5 for various settings of the energy analyzer. The energy values given for the individual scans in Fig. 5 represent the minimum separation energy that photofragments must possess to be transmitted through the energy analyzer. The energy discrimination shows conclusively that the dominant transitions which lead to the formation of the bandlike feature arise from C^+ photofragments with low separation energies $W < 20$ meV. These transitions disappear at the higher-energy settings, unveiling the presence of isolated transitions, similar to those in the red part of the spectrum of Fig. 4.

The separation energy W was measured explicitly for approximately 100 transitions by setting the laser to the observed transition and scanning the energy analyzer. Figure 6 shows two typical kinetic-energy spectra. The separation energy in the center-of-mass frame is obtained from the half-width of the spectra measured at half-height, as indicated by the arrows. In this way the value of 100 ± 10 meV is obtained for both spectra in Fig. 6. As will be shown later, the transitions pumped here access the two Λ-doubling components of the shape resonance $v'=1$, $J'=32$ in the A state, the two components lying 102.9 and 105.2 meV, respectively, above the dissociation limit $C^+(^2P_{3/2})+H(^2S)$. In the center-of-mass frame the separation energy is a rather well-defined quantity. If fragmentation occurs to a single dissociation limit, the intrinsic uncertainty in W is introduced through the finite lifetime of the quasibound level. As will be shown later this uncertainty amounts to about 10^{-5} cm^{-1} for the two levels considered in Fig. 6. The observation of a rather broad energy distribution as measured by the energy analyzer in the laboratory frame is caused primarily by three effects: the angular distribution of photofragments with respect to the laser polarization, the energy inhomogeneity of the parent-ion beam ($\Delta E_{lab}\sim1$ eV), and the finite resolution of the energy analyzer ($\Delta E_{lab}\sim1.5$ eV). The latter two effects are clearly small contributions to the broad distribution, as may be judged from the laboratory-energy scales shown along the upper abscissas in Figs. 6(a) and 6(b).

The angular distribution of the photofragments in the center-of-mass frame, however, translates the well-defined center-of-mass separation energy into a specific laboratory-energy distribution, the transformation being determined by the separation energy

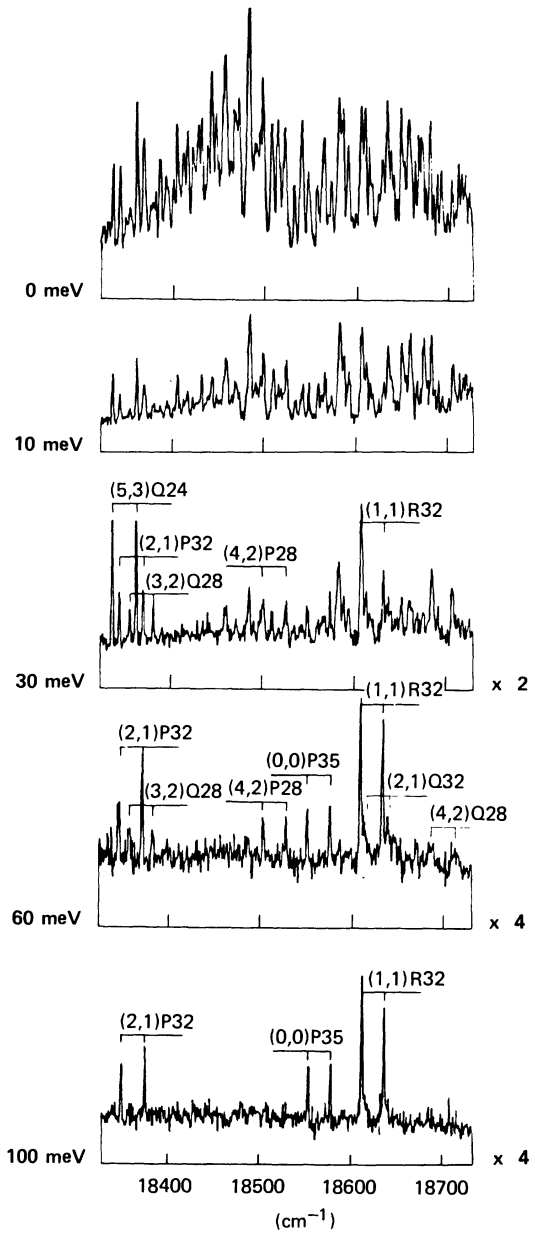

FIG. 5. Portion of the spectrum of Fig. 4 obtained at various settings of the energy analyzer. The energies given for the individual scans denote the minimum separation energies photofragments must possess to be transmitted through the energy analyzer.

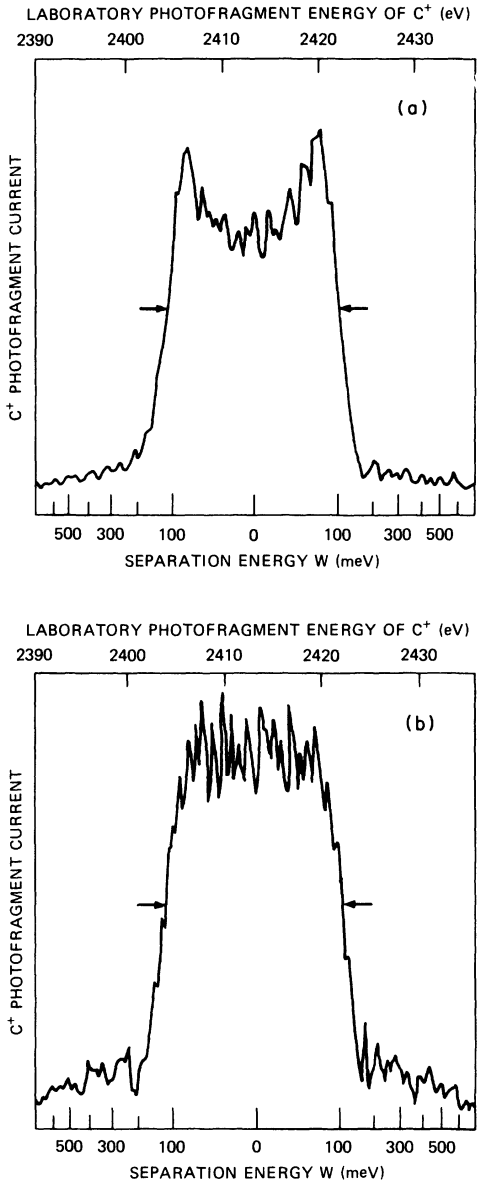

FIG. 6. Photofragment kinetic-energy spectra for predissociation of CH^+ $A\,^1\Pi$ $v'=1$, $J'=32$. In (a) the exciting transition is $(1,1)Q\,32$; the exciting transition in (b) is $(1,1)P\,33$.

and the solid angle under which the aperture to the energy analyzer is viewed from the region of predissociation. The angular distribution in the center-of-mass frame itself is characteristic for the symmetry of the transition pumped and the predissociation lifetime.[21] For the spectra in Fig. 6 the exciting transitions are $(1\leftarrow1)Q(32)$, and $(1\leftarrow2)R(31)$, respectively. The drastic difference in the two distributions arises from the different ΔJ values in the exciting transitions, as previously explained by Pernot *et al.*[26] For a perpendicular transition, such as represented by the Q branch of the $A\,^1\Pi\leftarrow X\,^1\Sigma^+$ system at high values of J, the distribution is predicted and observed to exhibit a distinct minimum in the photofragment signal at $W=0$, while it is less pronounced or even a max-

imum at $W=0$ for transitions in the P and R branches. This characteristic was very valuable in the identification of the observed transitions.

V. IDENTIFICATION OF THE SHAPE RESONANCES

Shape-resonance levels in the A state exist for a very select range of rotational and vibrational levels. Our photofragment-spectroscopy experiment is based on the observation of absorption lines leading to shape resonances which predissociate in times less than about 10 μs (the residence time of ions in the laser interaction region). These transitions therefore appear without the band-forming structure which generally assists in the assignment of rotational lines in molecular-absorption spectra, since only a few rotational levels (sometimes only one) are quasibound for a given value of v'. Adding to this complication is the fact that rotationally quasibound levels for a given value v' are not regularly spaced, due to the strong anharmonicity of the potential-energy curve describing the shape resonances (Fig. 2).

A. Existing spectroscopy of CH^+

Since the discovery of the $A \leftarrow X$ emission system by Douglas and Herzberg[27] a number of high-resolution emission studies have been undertaken for this system in both CH^+ and CD^+. For CH^+ these studies have covered the $v''=0$ and 1 progressions up to $v'=2$, $J'=10$ and $v'=4$, $J'=7$, respectively.[27,28] Grieman, Mahan, O'Keefe, and Winn[23] succeeded in extending the high-resolution study for the (0,0) band in CH^+ up to $J'=22$ using laser-induced fluorescence with hot CH^+ in an ion trap. Similarly high rotational levels were observed in low-resolution emission studies of CH^+ produced in the chemiluminescent ion-molecule reaction $C^+ + H_2$ by Kusunoki and Ottinger.[29] Figure 7 shows the energy location of the rotational levels observed in spectroscopic studies with respect to the dissociation limit. The shape-resonance levels of the A state and the levels in the X state from which the dissociating transitions originate, also indicated in this figure, occur at much higher rotational and vibrational levels than were sampled in previous studies. The shape resonance levels of the A state are not amenable to an extrapolation from low rotational levels because of the anharmonicity of the potential well; consequently, an unambiguous correlation of the observed transitions to shape resonances with those from previous studies does not follow immediately. The photon energy of a particular transition, combined with the measured photofragment energy, allows the calculation of the energy of the X-state level with respect to the dissociation limit. As indicated in Fig. 7, some of the uv transitions to shape resonance sample the X state at energies where previous information is indeed available. Even for these transitions, however, no immediate assignment of the upper and lower rovibrational levels may be made because of the following:

(a) The dissociation energy of $CH^+ X\,^1\Sigma^+$ is uncertain by ± 180 cm^{-1}: the currently accepted value,[13] derived in a thermodynamic cycle involv-

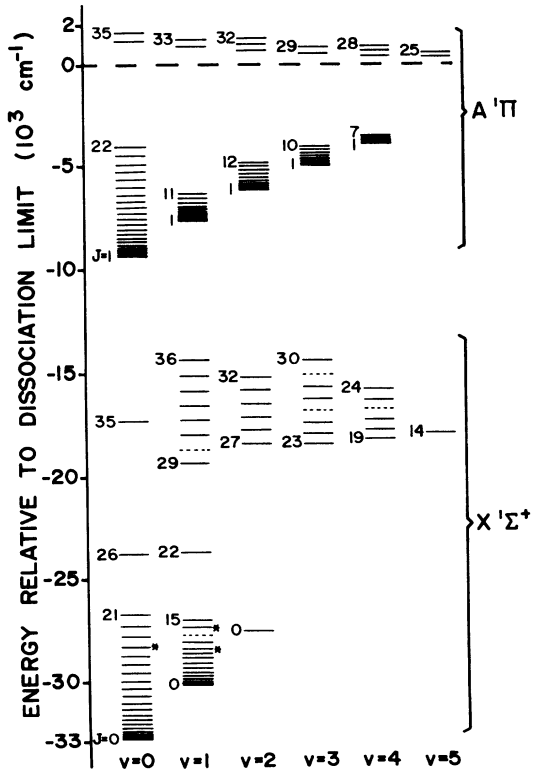

FIG. 7. Molecular energies for terms observed in the X and A states of CH^+ for vibrational quantum numbers $0 \le v \le 5$. Previous high-resolution studies have observed the low rotational levels ($J'' \le 21$ in the X state and $J' \le 22$ in the A state). In the present work the shape-resonance levels (indicated above the dissociation limit $E=0$) were pumped from the high rotational levels in the X state. In addition, transitions from the lower rotational levels indicated by an asterisk to shape-resonance levels were also observed.

ing the dissociation energy[30] and the ionization potential[31] of CH, is limited by the uncertainty in those values (80 and 100 cm^{-1}, respectively).

(b) Experimental values of W have an uncertainty of typically $\pm 10\%$.

(c) Shape resonances might decay into the $C^+(^2P_{3/2})+H(^2S)$ or the $C^+(^2P_{1/2})+H(^2S)$ limit, adding as additional uncertainty the fine-structure splitting[32] of $C^+(^2P)$ (63.42 cm^{-1}).

Consequently, neither the rotational nor the vibrational quantum numbers of these quasibound states may be easily deduced from the observed photofragments. This problem was also encountered by Carrington and Sarre[33] who observed two predissociated levels in CH^+.

The key to the identification of the observed transitions was the knowledge of the separation energies from kinetic-energy spectra such as those shown in Fig. 6. The general characteristics of the observed photofragment kinetic energies up to ~ 200 meV were quite different from the predictions[4,11] based on *ab initio* potential curves,[34] for which the highest shape resonance occurred at only 140 meV, but were in agreement with those calculated by Graff and Moseley[12] who used an empirical potential. This is due primarily to the fact that, as verified here, the well depth of the A state, 1.27 eV, is much larger than the *ab initio* prediction of 1.07 eV.[6,34] The analysis of the observed transitions and corresponding photofragment energies, therefore began with a study of the two potential curves involved.

B. $X\,^1\Sigma^+$-state potential

The ground state $X\,^1\Sigma^+$ is well characterized only near the potential minimum, only the two lowest vibrational levels having been observed by high-resolution emission spectroscopy.[27,28] The band oscillator strengths for low rotational levels in the $A \rightarrow X$ system strongly favor transitions to $v''=0$ and $v''=1$ for molecules in the lower vibrational levels of the A state. Consequently, it is only these bands for which emissions studies have been reported. The majority of transitions observed in the present photodissociation study sampled a region of the X state that is about 1.5 eV above the region characterized by the high-resolution data, so that even the most reliable existing molecular constants could provide only a rough indication of the relative spacings of the high rotational levels involved in these transitions, while the absolute locations of these levels could not be accurately predicted at all.

In constructing a trial potential for the X state, Graff and Moseley[12] performed an RKR calculation using the vibrational constants of Douglas and Morton[28] and the rotational constants of Kusunoki and Ottinger.[29] The resulting curve provided the lower 2.5 eV of the X-state potential. To establish the depth of the well, they used the currently accepted value[13] of the CH^+ dissociation energy $D_0^0=4.085\pm.022$ eV. To complete the curve, the long-range behavior ($R>2.65$ Å) given by Launay and Roueff,[9] and the repulsive inner wall of the potential given by the *ab initio* calculation of Green *et al.*,[34] both appropriately adjusted to conform to the dissociation energy above, were used.

Here, the rovibrational eigenvalues were calculated for this potential with various potential forms at intermediate ($1.87<R<2.65$ Å) internuclear distance using a program by LeRoy.[35] In addition, since it was necessary to apply an RKR calculation far above its region of spectroscopic accuracy, the magnitude of the uncertainty in the extrapolation was estimated by calculating the RKR potential curves and corresponding eigenvalues using the several available sets of vibrational constants.[36–38] The spacings of rotational levels at high J for these potentials were compared, as were the relative positions of high rotational levels for various vibrational states, and the resulting patterns were used as a gauge in assigning the observed transitions. Using the calculated quasibound levels in the A state as a pattern and assuming that the rotational levels of the X state would exhibit a pattern similar to those calculated from the potentials described above, analysis began with transitions to the lowest vibrational levels of the A state. These give rise to photofragments with the highest separation energies. Since these levels are relatively few in number they were most easily assigned. In addition, the calculation of the shape-resonance levels[4,11,12] indicated that for most vibrational states there are typically only two rotationally quasibound levels that would be expected to dissociate and be detected in this experiment: levels wider than 20 cm^{-1} would provide a signal too diffuse for detection, and levels narrower than 10^{-6} cm^{-1} would not dissociate during the ion flight time.

C. Oscillator strengths

A consistent assignment of 14 transitions in the (0,0), (0,1) and (1,1) bands indicated that the X state was adequately described by our trial potential for the purposes of the assignment of the excitation spectrum. Using a polynomial fit to the transition moment $M(R)$ given by Elander, Od-

dershede, and Beebe,[39] the oscillator strengths

$$f_{v',v''}(J',J'') = \frac{4}{3}\Delta E \,|\, \langle \phi_{v'J'}(R) \,|\, M(R) \,|\, \phi_{v''J''}(R) \rangle \,|^2 \tag{5.1}$$

were calculated for all transitions in the examined wavelength range which would terminate on quasibound levels observable in this study. Table I shows the results of this calculation. The oscillator strengths were invaluable in completing the assignments for higher vibrational levels of the A state, since some bands, such as the (2,2), are predicted to be too weak to be observed at these high rotational levels.

As may be seen in Table I, most of the transitions with oscillator strengths of about 5×10^{-5} or greater within the investigated wavelength range were observed. Transitions with lower oscillator strengths, with the exception of lines in the uv range, were apparently too weak to be observable. In addition, there are several transitions which

TABLE I. Transition energies in cm^{-1} and oscillator strengths in atomic units for transitions to shape resonances of the $A\ ^1\Pi$ state of CH^+ from the $X\ ^1\Sigma^+$ state in the energy range 16000–19600 cm^{-1}. Transitions to shape resonances which are predicted, but were not observed in this study, are not included.

(v',v'')	J''	P	$f(P)\times10^3$	Q	$f(Q)\times10^3$	R	$f(R)\times10^3$
(0,0)	34			19306[a]	0.121		
	35	18556.2	0.131	18904.0	0.046		
	36	18148[a]	0.050				
(0,1)	33					17864.3	0.218
	34			17115.5	0.222	17509.2	0.096
	35	16397.5	0.226	16745.5	0.099		
	36	16022.0	0.102				
(1,0)	34	19361[a]	0.346				
(1,1)	31					1890.0	0.462
	32			18259.9	0.437	18616.1	0.359
	33	17564.3	0.408	17881.0	0.348		
	34	17168.8	0.333				
(1,2)	31					16813.5	0.162
	32			16130.7	0.135	16482.6	0.187
(2,1)	30			19430[a]	0.163		
	31	18759[a]	0.121	19046.0	0.224		
	32	18362.3	0.184	18617.0	0.237		
	33	17924[a]	0.208				
(2,2)	29					17903[a]	0.012
	30			17235[a]	0.022	17558[a]	0.002
	31	16592[a]	0.034	16787[a]	0.000	17174[a]	0.028
	32	16232[a]	0.002	16487[a]	0.017		
(3,1)	30	19568[a]	0.000				
(3,2)	27					19014[a]	0.246
	28			18372.6	0.250	18660[a]	0.151
	29	17754.9	0.248	18003.2	0.163		
	30	17372.9	0.172				
(3,3)	27					16845.5	0.102
	28			16235.1	0.082	16522.3	0.120
(4,2)	26			19480[a]	0.184		
	27	18889[a]	0.147	19116.0	0.201		
	28	18510.2	0.174	18697.0	0.163		
	29	18081[a]	0.150				
(4,3)	25					17859[a]	0.004
	26			17282[a]	0.011	17542[a]	0.003
	27	16721[a]	0.021	16947[a]	0.000	17173[a]	0.022
	28	16373[a]	0.001	16560[a]	0.013		
(5,3)	23					18904.0	0.145
	24			18354.8	0.154	18555[a]	0.074

TABLE I. (*Continued.*)

(v',v'')	J''	P	$f(P)\times10^3$	Q	$f(Q)\times10^3$	R	$f(R)\times10^3$
	25	17821.9	0.159	17992.9	0.086		
	26	17443.0	0.096				
(5,4)	23					16758.4	0.66
	24			16242[a]	0.052	16442.7	0.074
(6,3)	22			19354[a]	0.142	19528[a]	0.117
	23	18854[a]	0.121	18991[a]	0.110		
	24	18472.0	0.100				
(6,4)	22					17372[a]	0.004
	23			16845[a]	0.001		
	24	16359[a]	0.000				
(7,4)	18					18858[a]	0.095
	19			18421.5	0.101	18556.2	0.046
	20	17990.3	0.104	18102.5	0.053		
	21	17655.3	0.058				
(7,5)	18					16715[a]	0.032
	19			16293[a]	0.024	16428[a]	0.035
(8,4)	16					19636[a]	0.084
	17			19236[a]	0.078		
	18	18846[a]	0.071				
(8,5)	16					17464[a]	0.000
	17			17078[a]	0.001		
	18	16702[a]	0.002				
(9,5)	13					18416[a]	0.022
	14			18092.7	0.024		
	15	17774[a]	0.027				
(9,6)	13					16262[a]	0.015
(10,5)	11					18935[a]	0.014
	12			18657[a]	0.014		
	13	18376[a]	0.014				
(10,6)	11					16761[a]	0.001
	12			16493[a]	0.001		
	13	16222[a]	0.001				
The following transitions were also observed:							
(4,0)	26			24180.8	0.807		
(7,0)	18					28464.0	0.106
(8,0)	18	28448.2	0.024				
(2,1)	29					20122.6	0.207
(6,1)	22					24183.0	0.431
(9,1)	14			27498.9	0.089		
(10,1)	11					28484.3	0.023
(2,3)	30					15459.9	0.053

[a]Calculated photon energies of transitions not observed in this study: uncertainties are approximately ±10 cm^{-1} for transitions to levels $v'\leq4$, ±30 cm^{-1} for $v'\geq5$.

were not observed, despite favorable oscillator strengths. Reasons for this are as follows:

(a) Many peaks with transition energies greater than about 18500 cm^{-1} were not observed due to the dense manifold of near-threshold [group (a)] photodissociations occurring in this wavelength range (Fig. 4) which obscured the shape-resonance photofragments.

(b) In two cases, $(2,1)P33$ and $(4,2)P29$, a transition to the e level of a Λ doublet is not observed,

although transitions to the corresponding f levels are observed. In each of these cases the linewidth of the f-level transitions was rather large. We suspect that the e levels will exhibit even larger linewidths making them unobservable.

(c) The transitions $(5,4)Q24$ and $(5,3)P26$, which lie at the edge of the dye-laser range for Rhodamine 6G, were not observed due to weak laser intensity at these wavelengths.

Several transitions for which we predict small oscillator strengths appear in the spectrum. These originate from the lower rovibronic levels of the X state, the low oscillator strength value being counterbalanced by a higher population in these levels.

VI. RESULTS AND DISCUSSION

A. Identification of shape resonances

Assignments are made for 32 Λ-doublet components of 21 different rovibrational levels of the A state which predissociate. The transitions to these levels originate from 31 rovibrational levels of the X state. The $v''=1$ level of the X state is the most fully characterized by the assigned transitions, with seven high rotational levels ($J''=29$ and $31-36$) fixed by a connected set of transitions in the (0,1) and (1,1) bands, and three somewhat lower rotational levels ($J''=11$, 14, 22) that were accessed by transitions in the uv range.

B. Rotational constants and dissociation energy

The (0,1) and (1,1) bands are well characterized at high rotational levels by this study, six transitions to rotationally quasibound levels having been observed for each band. By combining these upper portions of the bands with the observations of Douglas and Morton[28] at low rotational levels, we calculated the corresponding molecular constants for each band. The results for these two bands were then merged to provide the rotational constants presented in Table II. The $X\,^1\Sigma^+$ state for $v''=1$ is adequately described for $J''=0-36$ using rotational constants B_1'', D_1'', and H_1''. Owing to the high anharmonicity of the $A\,^1\Pi$ state, the constant L_v' was added to the constants B_v', D_v', and H_v' to improve the characterization of the high rotational levels of $v'=0$ and 1. A second-order Λ-doubling constant, qd_v, was needed in addition to the first-order constant q_v to describe this splitting for high rotational levels. The definition of the constant in Table II follows the convention of Zare *et al.*[40] These constants match the data of Douglas and Morton[28] with an uncertainty of ± 0.033 cm^{-1} which is an improvement in the fit. They match the transitions to shape resonances observed in this study to within ± 8 cm^{-1}. The experimental line positions for the transitions to the shape-resonance levels reported here have an experimental uncertainty of ± 1 cm^{-1}. The larger uncertainty in the fitting of the shape-resonance levels is attributed to the difficulty in properly describing

TABLE II. Molecular constants (cm^{-1}) for the $X\,^1\Sigma^+$ and $A\,^1\Pi$ states of CH^+.

$X\,^1\Sigma^+$		$v=1$
B_v		13.4427(7)[a]
D_v		$1.352(7)\times10^{-3}$
H_v		$9.6(5)\times10^{-8}$
$D_0^0(X\,^1\Sigma^+)=32\,907(23)$ [relative to $C^+(^2P_{1/2})+H(^2S)$]		
$A\,^1\Pi$	$v=0$	$v=1$
B_v	11.4067(8)	10.4626(7)
D_v	$1.993(8)\times10^{-3}$	$2.088(7)\times10^{-3}$
H_v	$0.42(20)\times10^{-7}$	$1.09(21)\times10^{-7}$
L_v	$-1.7(2)\times10^{-10}$	$-2.3(2)\times10^{-10}$
q_v	0.0388(3)	0.0357(2)
qd_v	$-1.6(2)\times10^{-5}$	$-1.8(2)\times10^{-5}$
$D_0^0(A\,^1\Pi)=9351(23)$ [relative to $C^+(^2P_{3/2})+H(^2S)$]		

[a]Numbers in parentheses represent an uncertainty of one standard deviation in the final digits of each number.

molecular energies close to the dissociation barrier with a limited set of parameters.

These improved rotational constants for the vibrational level $v''=1$ of the $X\,^1\Sigma^+$ state establish the energy separation of the high rotational levels from the level $J''=0$, whose separation from $(v''=0, J''=0)$ is known from high-resolution spectroscopy. By combining the photon energy of transitions from these high rotational levels with the measured kinetic energies of the resulting photofragments, it was possible to determine the dissociation energy of CH^+. Although the measured photofragment kinetic energy for any individual transition is known only to an accuracy of about 10%, the complete set of 52 transitions taken together provides a much more accurate measure of the separation of the observed set of rotationally quasibound levels from the dissociation limit.

A preliminary assignment of shape-resonance energies was made under the constraint that the assignments be consistent with all observed transitions. For each transition to vibrational levels $0\le v'\le 8$, the difference between the measured photofragment kinetic energy and the energy assigned to its terminal level was calculated. Weighting each of these offsets by the inverse square of the uncertainty in the kinetic-energy measurement, the weighted average offset was determined, and the energy placement of the set of shape resonances was chosen so that the average offset was zero. For vibrational levels $v'=0-8$ $(J'\ge 17)$, the calculation indicated that all transitions resulted in dissociation to a single dissociation limit. As will be shown later we identify this dissociation limit as $C^+(^2P_{3/2})+H(^2S)$.

The uncertainty in the value for the dissociation energy determined here arises primarily from two sources: (1) The uncertainty in the separation of the high rotational levels of $v''=1$ from $(v''=1,J''=0)$, which may be calculated using the variance-covariance matrix[41] of the merged constants

$$\sigma^2\{E(J'')-E(0)\}=\mathrm{var}(B)J''^2(J''+1)^2+\mathrm{var}(D)J''^4(J''+1)^4+\mathrm{var}(H)J''^6(J''+1)^6$$
$$+2\,\mathrm{cov}(B,D)J''^3(J''+1)^3+2\,\mathrm{cov}(B,H)J''^4(J''+1)^4+2\,\mathrm{cov}(D,H)J''^5(J''+1)^5\ .$$

For $J''=34$, the center of the high-J levels used in the merged constants calculation

$$\sigma^2\{E(34)-E(0)\}=(17.9\ \mathrm{cm}^{-1})^2\ .$$

(2) The uncertainty in the separation of the high rotational levels of $v''=1$ from the dissociation limit, which is deduced from the kinetic energy of the photofragments and the corresponding transition energy, and may be calculated using the sample standard deviation of the weighted average offset calculation described above:

$$s^2(\bar{x})=\frac{1}{n-1}\frac{\sum(x_i-\bar{x})^2/\sigma_i^2}{\sum 1/\sigma_i^2}=(4.7\ \mathrm{cm}^{-1})^2\ ,$$

where $\bar{x}$ is the weighted average offset $(W_{\mathrm{assign}}-W_{\mathrm{obs}})$, x_i is the offset of the ith transition, and σ_i is the uncertainty in the kinetic-energy measurement $\sigma_i=0.1\times W_{\mathrm{obs}}$.

The separation of $(v''=0,J''=0)$ from $(v''=1,J''=1)$ is well known from high-resolution spectroscopy,[27] and contributes a negligible uncertainty to this calculation. Combination of these two factors provides an uncertainty of

$$\sigma(D_0)=[\sigma^2\{E(34)-E(0)\}]^{1/2}+[s^2(\bar{x})]^{1/2}$$
$$=23\ \mathrm{cm}^{-1}\ .$$

As a result of this calculation, we obtain for the dissociation energy

$$D_0^0(CH^+\,X\,^1\Sigma^+ v=0,J=0)$$
$$=32\,907\pm 23\ \mathrm{cm}^{-1}\ , \quad (6.1)$$

measured relative to the $C^+(^2P_{1/2})+H(^2S)$ dissociation limit. This value, which is within the 180-cm^{-1} limits discussed in Sec. V of the value 32 947 cm^{-1} given by Huber and Herzberg,[13] is a substantial improvement in our knowledge of the bond energy of this molecule.

From the observed energy of the (0,0)R 0 line in the $A\rightarrow X$ system, and the fine-structure splitting in $C^+(^2P)$, the dissociation energy of the lowest existing level in the A state is

$$D_0^0(CH^+\,A\,^1\Pi v=0,J=1)=9351\pm 23\ \mathrm{cm}^{-1}, \quad (6.2)$$

relative to the $C^+(^2P_{3/2})+H(^2S)$ dissociation limit.

Since the ionization potential of CH has been determined to be $85\,850\pm100$ cm^{-1},[31] the dissociation energy of the ground state of CH $X\,^2\Pi$ relative to its adiabatic dissociation limit $C(^3P_0)+H(^2S)$, can be determined in a thermodynamic cycle using the dissociation energy of CH^+ obtained in this study and the ionization energy of carbon[32]:

$$D_0^0(\mathrm{CH}\,X\,^2\Pi v=0,J=\tfrac{1}{2})=27\,937\pm123\ \mathrm{cm}^{-1}. \tag{6.3}$$

This value is in agreement with the value of $27\,950\pm80$ cm^{-1} obtained by Brzozowski, Bunker, Elander, and Erman[30] in a predissociation study of the $B\,^2\Sigma^-$ state of CH.

C. Comparison of assignments with calculation

The empirical potentials for the X and A states described previously were further adjusted to reflect the improved dissociation energy and provide better comparison with experiment. The resulting potential curves are given by Table III. We then calculated the eigenvalues for these potentials, including the energies and widths of the rotationally quasibound levels, using the LeRoy program.[35] The results of this calculation for the A-state shape resonances are shown in Table IV, together with the assigned energies of shape resonances observed in this study. The available linewidth measurements for these levels are also given in this table. With the exception of the single-mode laser measurements made at the ion-laser lines and several broad shape resonances observed at visible wavelengths, the linewidths of most transitions fell within the ~1 cm^{-1} dye-laser bandwidth and are not reported.

A graphic comparison of our assigned A shape-resonance energies with those calculated for the potential of Table II is presented in Fig. 3(b). The agreement for lower vibrational levels is very good. The difference between the observed levels and those calculated is generally greatest for the higher vibrational levels. This may be due to the form of the potential chosen at intermediate internuclear separation.

A comparison of measured and calculated linewidths shows only qualitative agreement. This is to be expected since the linewidths are extremely sensitive to the long-range part of the interaction potential. No attempt was made to adjust this part of the potential to obtain better agreement with the measured linewidths. Once the lifetimes of more shape resonances have been established experimentally it will be feasible to deduce the potential at very large R values from such data.

D. Λ doubling

Electronic terms with $\Lambda>0$ are twofold degenerate in the absence of rotation. This degeneracy is removed in the rotating molecule due to the incipient decoupling of the orbital angular momentum vector from the internuclear axis to the axis of rotation. For scattering of $C^+ + H$ along the $A\,^1\Pi$ potential curve, the following simplified picture may be drawn to explain the dynamic origin of the observed Λ doubling in the A state: In Fig. 8 we consider the interaction of the carbon ion and hydrogen atom at large internuclear distances in terms of the possible orientations of the $2p$ orbital of the carbon ion with respect to the z axis, which connects the carbon and hydrogen nuclei. Effects introduced by the electron spin are neglected and the y-z plane is taken as the plane of rotation. The p_z atomic orbital [Fig. 8(a)] will lead to the formation of a Σ state, the p_x and p_y orbitals to a doubly degenerate Π state. If the electrons were able to follow the nuclear motion exactly, with no lag or slip,[42] the two π orbitals would have precisely the same energy. Since the electrons cannot follow the motion of the nuclei exactly, there is a tendency for them to lag behind the motion of the nuclei. This has virtually no effect in the state formed from the p_x orbital [Fig. 8(b)]. For the p_y orbital [Fig. 8(c)], however, it is easy to see that the electron slip leads to a configuration which has partly σ character. Similar considerations hold for the p_z orbital which ends up with partly π character. The distinction between σ and π orbitals becomes increasingly blurred with increasing speed of rotation, thus lifting the degeneracy in the $^1\Pi$ state. In a quantum-mechanical treatment the Λ doubling is obtained as a rotational perturbation of the $^1\Pi$ state by neighboring $^1\Sigma$ states. The lowest $^1\Sigma^-$ state in CH^+ appears 10.2 eV above the lowest dissociation limit; hence the much closer $^1\Sigma^+$ states will be the dominant origin for the observed Λ doubling of the $A\,^1\Pi$ state.

To our knowledge this effect is often neglected in scattering calculations due to the small magnitude of the Λ doubling (generally less than a few meV). For processes which are dominated by shape resonances, however, inclusion of Λ doubling

TABLE III. CH^+ potential-energy curves obtained in this work. For the $X\,^1\Sigma^+$ state the energies are relative to $C^+(^2P_{1/2})+H(^2S)$. For the $A\,^1\Pi$ state the energies are relative to $C^+(^2P_{3/2})+H(^2S)$.

$X\,^1\Sigma^+$		$A\,^1\Pi$	
R(Å)	$V(R)$ (cm^{-1})	R(Å)	$V(R)$ (cm^{-1})
0.741	6816.88	0.794	21 238.56
0.794	−6979.29	0.926	1362.94
0.840	−14 884.83	0.977	−3977.99
0.848	−17 035.71	0.984	−4489.91
0.859	−19 238.40	0.993	−5043.92
0.874	−21 506.87	1.003	−5641.99
0.892	−23 855.12	1.016	−6286.11
0.916	−26 297.15	1.032	−6978.25
0.947	−28 846.93	1.052	−7720.40
0.994	−31 518.48	1.078	−8514.53
1.030	−32 904.28	1.116	−9307.53
1.057	−33 610.45	1.147	−9807.53
1.131	−34 323.81	1.234	−10 265.70
1.217	−33 610.45	1.346	−9807.53
1.256	−32 904.28	1.402	−9362.63
1.318	−31 518.48	1.493	−8514.53
1.415	−28 846.93	1.575	−7720.40
1.500	−26 297.15	1.654	−6978.25
1.579	−23 855.12	1.732	−6286.11
1.654	−21 506.87	1.811	−5641.99
1.727	−19 238.40	1.892	−5043.92
1.797	−17 035.71	1.977	−4489.91
1.865	−14 884.83	2.064	−3977.99
2.646	−3202.14	2.696	−1485.39
3.440	−520.59	2.899	−1004.00
4.500	−114.73	3.100	−720.00
5.500	−47.01	3.200	−600.00
6.500	−23.36	3.440	−386.39
8.000	−9.93	4.000	−196.64
10.000	−4.00	4.500	−116.98
15.000	−0.78	5.000	−73.97
20.000	−0.24	5.500	−49.11
		6.000	−33.91
		6.500	−24.19
		8.000	−10.18
		10.000	−4.06
		15.000	−0.78
		20.000	−0.25

appears mandatory. In the present case Λ doubling leads to nearly a twofold increase in the number of resonances (in a few cases only one Λ-doubling component is quasibound). The doubling is observed for a number of shape resonances; its magnitude is comparable to the energy spacing of individual resonances belonging to different vibrational levels (see Table IV). Since the predissociation lifetimes (i.e., the energetic width of the shape resonances) depends critically on the energy location of the quasibound levels, the two Λ-doubling components of a resonance should appear with different widths. Unfortunately, the currently available linewidth data are not extensive enough to confirm this effect experimentally. A theoretical calculation which includes the effect of Λ doubling

TABLE IV. Comparison of assigned shape-resonance energy levels with those calculated for the $A\ ^1\Pi$ potential curve used in this study. Uncertainties for observed levels with $v'=0-4$ are $\pm 5\ cm^{-1}$ relative to each other and the uncertainty in the separation of the set of levels from the dissociation limit is $\pm 9\ cm^{-1}$. For observed levels with $v' \geq 5$, the relative uncertainties are $\pm 10\ cm^{-1}$, with an uncertainty of $\pm 20\ cm^{-1}$ for the separation of the set of levels from the dissociation limit. The energies are relative to the $C^+(^2P_{3/2})+H(^2S)$ dissociation limit. Energies and widths are given in cm^{-1}.

		CALC.		EXPT.			
				e component		*f* component	
v	J	Energy	Width	Energy[a]	Width[b]	Energy[a]	Width[b]
0	36	1798.0	36.9				
0	35	1481.3	0.39	1524.0		1498.5	
0	34	1120.2	2.9(−4)	1150.3		1128.9	
0	33	727.8	2.5(−9)				
0	32	313.2	5.3(−20)				
1	34	1446.3	16.1				
1	33	1140.7	9.4(−2)	1184.2		1166.6	
1	32	809.3	2.9(−5)	848.8		830.0	
1	31	459.9	1.3(−11)				
1	30	96.3	1.2(−30)				
2	32	1172.5	10.6			1187.1	~12
2	31	891.1	5.8(−2)	932.1	≤0.11	913.6	
2	30	589.6	6.0(−6)	626.8	0.01		
2	29	276.0	3.1(−14)				
3	30	959.4	14.5				
3	29	708.4	9.1(−2)	746.6	~4.5	726.9	
3	28	440.6	3.8(−6)	477.5		459.4	
3	27	163.2	2.2(−16)				
4	28	796.6	30.1			783.8	~13
4	27	579.7	0.35	597.0		579.3	<1.1
4	26	345.3	2.0(−5)			337.7	
4	25	103.1	2.6(−17)				
5	26	667.3	241.7				
5	25	491.0	4.0	503.7	≤2	486.3	
5	24	293.5	5.6(−4)	314.9		303.1	
5	23	86.1	6.3(−15)				
6	23	420.6	37.7	420.3	≳2		
6	22	266.9	9.7(−2)				
6	21	98.2	1.7(−9)				
7	20	243.4	9.5	220.4	≲2.3	210.1	<2.5
7	19	118.1	4.7(−4)	97.9	8.0(−3)	85.7	
8	17	127.0	2.7	82.1			
8	16	32.1	1.5(−8)				
9	14	56.7	0.79			32.1[c]	5.2(−2)
10	12	41.1	41.8	4.4[c]	0.433		
10	11	11.1	5.8(−4)				
11	9	11.5	1.3				
13	4	0.6	6.9(−2)				

[a]Experimental energies given are the results from the final data analysis. These values fall within the ±10% absolute uncertainty of the raw experimental separation energy measurements.

[b]Level widths which are not given explicitly are $<2\ cm^{-1}$.

[c]The kinetic-energy spectra of the photofragments from these levels suggest unresolved contributions to both $C^+(^2P)$ spin components in the dissociation.

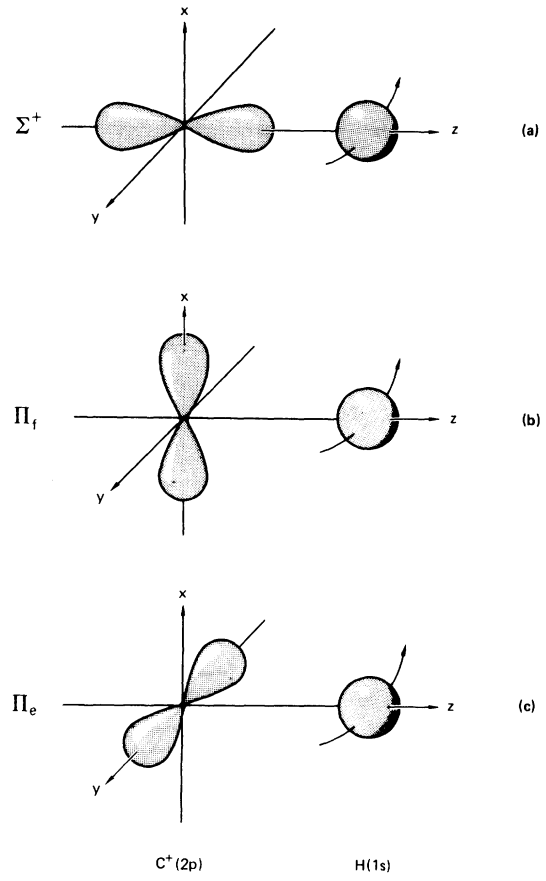

FIG. 8. Molecular-orbital picture showing qualitatively the origin of Λ doubling in the $A\ ^1\Pi$ and $X\ ^1\Sigma^+$ states of CH^+.

on the shape-resonance levels and which also predicts the centrifugal distortion and vibrational dependence of the Λ splitting will be presented in a separate paper.[43]

E. Predissociation mechanism

In the absence of other nearby electronic states, shape-resonance levels can predissociate only by tunneling through the rotational barrier. In the current case this will lead to population of the fine-structure limit $C^+(^2P_{3/2})+H(^2S)$ (see Fig. 1). However, a complication may arise due to competition between this barrier penetration and predissociation by spin-orbit and rotational coupling. The predissociating levels of the $A\ ^1\Pi$ state studied here may, in principle, be classified into two groups, according to their possible means of predissociation: (a) Shape resonances near the rotational barrier maxima will predissociate rapidly by barrier penetration, their short lifetimes making other types of predissociation unlikely. Similarly, shape-resonance levels which also lie below the corresponding rotational barriers of other electronic states are likely to predissociate only by penetrating the A-state barrier. A fine-structure transition to the lower dissociation limit $C^+(^2P_{1/2})+H(^2S)$ would be probable only at energies which coincide with shape resonance of both the A state and the second predissociating state. Since quasibound levels are sparse, this coincidence is rather unlikely. The transitions observed here, which correspond to shape resonances with $0 \leq v \leq 8$ ($17 \leq J \leq 35$), all yield photofragment kinetic-energy spectra which indicate that predissociation occurs to a single dissociation limit. Since most of these resonances lie well below the rotational barriers of the lower electronic states it is concluded that this dissociation limit is $C^+(^2P_{3/2}) + H(^2S)$. (b) Shape resonances of high vibrational levels all lie quite close to the barrier maximum, since they occur for lower rotational levels, which form small centrifugal barriers. At these low energies, however, the rotational barrier extends to large internuclear separations; hence the shape resonances are much narrower than with a similar depth below the barrier maximum for a lower vibrational (higher rotational) level. In this case, if a shape resonance lies above the corresponding rotational barrier of a lower electronic state, a fine-structure transition may result in more rapid dissociation (Mulliken case b_0 predissociation) since it couples to the continuum of the lower state. The branching ratio between the two fine-structure limits will depend on the relative lifetimes against barrier penetration and electronic predissociation. The $a\ ^3\Pi_{\pm 1}$ substate is the most likely lower-state candidate for such a predissociation[44] (see Fig. 1).

No observed transitions can be clearly shown to lead to dissociation primarily by such fine-structure transitions. However, the measured photofragment kinetic-energy spectra for predissociation from the quasibound levels ($v=9, J=14$) and ($v=10, J=12$), while poorly resolved, are consistent with what would be expected if both C^+ fine-structure levels were produced in their dissociation. This leaves open the possibility that both electronic and rotational predissociation are occurring in these levels. Further experimental work will be required to investigate this possibility.

F. Application to interstellar molecule formation

The observed abundances of CH and CH^+ in diffuse interstellar clouds have long posed a severe challenge to models of molecule formation. Even with the wealth of new experimental information involving the chemistry of these and related ions and neutrals, the discrepancy persists: all existing realistic models predict much less CH^+ in diffuse clouds compared to observations. Detailed reviews of the many considerations have been given.[45]

A major result of this study is the location and identification of rotationally quasibound levels which enhance the radiative association reaction (1.1). This will allow an improved calculation for this reaction. However, it is unlikely that this calculation will predict a sufficiently strong increase in the rate coefficient to make reaction (1.1) the dominant formation source of CH^+ in interstellar space. We would like to point out here that although Λ doubling leads to a nearly twofold increase in the absolute number of shape-resonance levels, this increase does not necessarily result in an increase in the rate coefficient, since the total collisional population of shape resonances is shared among two groups of opposite parity.

Also, a better characterization of the CH^+ X- and A-state potential curves and their bond dissociation energies, has been achieved in this study. Even though these potentials are not yet known to within the accuracy of the spectroscopic measurements, they nevertheless will allow an improved calculation of the direct photodissociation of CH^+ via the repulsive wall of the A state. Such a calculation may be warranted since it is now believed that CH^+ is formed in shock-heated regions.[46] Under these conditions it could be rotationally excited. In addition, more definitive investigations of other possible processes can be carried out. One is to attempt to explain the bandlike structures described in Sec. IV and shown in Figs. 4 and 5. If these arise from bound levels in the $A\ ^1\Pi$ state, which are predissociated to the $^2P_{1/2}$ limit, an additional mechanism for radiative association becomes available, as has been previously suggested.[25]

Finally, Kirby, Roberge, Saxon, and Liu[47] have calculated higher-lying states of CH^+, and predicted a total photodissociation rate at zero optical depth that is four orders of magnitude larger than dissociation only through the A state. Such a destruction rate would likely be important in determining the CH^+ abundance. Recalculation of the total destruction rate using the improved X-state potential curve is not warranted due to the uncertainty in the calculated dissociative potential curves. However, experimental observation of the processes predicted by Kirby *et al.*,[47] when combined with the X-state potential curve determined here, could lead to a clear identification of the states involved and an accurate determination of their location.

VII. CONCLUSION

Photofragment spectroscopy is applied to study the $A\ ^1\Pi$ state of CH^+ by selective excitation of shape-resonance levels in this state from $CH^+\ X\ ^1\Sigma^+$ with tunable laser radiation. Predissociation of the resonance levels in the A state is observed by measuring the appearance of C^+ fragments and their kinetic energies. The analysis of the excitation spectrum and the kinetic-energy distribution of the predissociation fragments has allowed the first experimental characterization of rotationally quasibound levels of the A state. At low collision energies ($\lesssim 200$ meV) these resonances decisively influence the radiative recombination and fine-structure changing cross section of $C^+ + H$. Our results are directly applicable in a theoretical treatment of these reactions. Λ doubling of the shape-resonance levels is observed. Refined molecular constants for the X and A states and the first direct experimental dissociation energy of CH^+, $D_0^0 = 4.080 \pm 0.003$ eV, are obtained.

ACKNOWLEDGMENTS

The authors would like to acknowledge a suggestion of Professor Alex Dalgarno, which initiated our study of CH^+. In addition, we had many helpful discussions with Professor Dalgarno and Dr. D. L. Huestis. The research work at SRI International was supported by SRI Internal Funds and in part by the National Science Foundation under Grants Nos. CHE-7700428 and PHY-8112548. The research at the University of Oregon was supported by the National Science Foundation under Grants Nos. AST-7918371 and CHE-7918074. Most of the computations were performed on a facility that was donated to the University by the M. J. Murdock Charitable Trust. One of us (H.H.), gratefully acknowledges a Max Kade fellowship during the early phases of this research.

[1]D. R. Bates, Mon. Not. R. Astron. Soc. 3, 303 (1951).
[2]P. Solomon and W. Klemperer, Astrophys. J. 178, 389 (1972).
[3]W. H. Smith, H. S. Liszt, and B. Lutz, Astrophys. J. 183, 69 (1973).
[4]A. Guisti-Suzor, E. Roueff, and H. van Regemorter, J. Phys. B 9, 1021 (1976).
[5]H. Abgrall, A. Guisti-Suzor, and E. Roueff, Astrophys. J. 207, L69 (1976).
[6]J. F. Bazet, C. Harel, R. McCarroll, and A. Riera, Astron. Astrophys. 43, 223 (1975).
[7]R. H. Garstang, J. Res. Natl. Bur. Stand. 68A, 61 (1964).
[8]A. Dalgarno and J. H. Black, Rep. Prog. Phys. 39, 573 (1976).
[9]J. -M. Launay and E. Roueff, J. Phys. B 10, 879 (1977).
[10]J. -M. Bazet, C. Havel, R. McCarroll, and A. Riera, Astron. Astrophys. 43, 229 (1975).
[11]T. Uzer and A. Dalgarno, Chem. Phys. Lett. 63, 22 (1979).
[12]M. M. Graff and J. T. Moseley, Chem. Phys. Lett. 83, 97 (1981).
[13]K. -P. Huber and G. Herzberg, *Molecular Spectra and Molecular Structure, Vol. 4, Constants of Diatomic Molecules* (Van Nostrand Reinhold, New York, 1979).
[14]H. S. W. Massey, *Electronic and Ionic Impact Phenomena* (Clarendon, Oxford, 1979), Vol. 3.
[15]S. Sinha, S. L. Lin, and J. N. Bardsley, J. Phys. B 12, 1613 (1979).
[16]G. Herzberg, *Molecular Spectra and Molecular Structure, Vol. 3, Spectra of Diatomic Molecules* (Van Nostrand Reinhold, New York, 1950).
[17]J. Schopman and J. Los, Physica (Utrecht) 48, 190 (1970).
[18]J. Schopman, P. G. Fournier, and J. Los, Physica (Utrecht) 63, 518 (1973).
[19]N. P. F. B. van Asselt, J. G. Maas, and J. Los, Chem. Phys. 5, 429 (1974).
[20]J. G. Maas, N. P. F. B. van Asselt, and J. Los, Chem. Phys. 8, 37 (1975).
[21]J. B. Ozenne, J. Durup, R. W. Odom, C. Pernot, A. Tabché-Fouhaillé, and M. Tadjeddine, Chem. Phys. 16, 75 (1976).
[22]B. A. Huber, T. M. Miller, P. C. Cosby, H. D. Zeman, R. L. Leon, J. T. Moseley, and J. R. Peterson, Rev. Sci. Instrum. 48, 1306 (1977).
[23]F. J. Grieman, B. H. Mahan, A. O'Keefe, and J. S. Winn, Faraday Disc. Chem. Soc. (in press).
[24]A. J. Lorquet, J. C. Lorquet, H. Wankenne, J. Momigny, and H. Lefebvre-Brion, J. Chem. Phys. 55, 4053 (1971).
[25]P. C. Cosby, H. Helm, and J. T. Moseley, Astrophys. J. 235, 52 (1980).
[26]C. Pernot, J. Durup, J. B. Ozenne, J. A. Beswick, P. C. Cosby, and J. T. Moseley, J. Chem. Phys. 71, 2387 (1971).
[27]A. E. Douglas and G. Herzberg, Can. J. Res. A 20, 71 (1942).
[28]A. E. Douglas and J. R. Morton, Astrophys. J. 131, 1 (1960).
[29]I. Kusunoki and C. Ottinger, J. Chem. Phys. 71, 4227 (1979).
[30]J. Brzozowski, P. Bunker, N. Elander, and P. Erman, Astrophys. J. 207, 414 (1976).
[31]G. Herzberg and J. W. C. Johns, Astrophys. J. 158, 399 (1969).
[32]C. E. Moore, *Ionization Potentials and Ionization Limits Derived From The Analysis of Optical Spectra*, Natl. Stand. Ref. Data Ser., No. 34 (Natl. Bur. Stand., Washington, D.C., 1970).
[33]A. Carrington and P. J. Sarre, J. Phys. (Paris) 40, C1-57 (1979).
[34]S. Green, P. S. Bagus, B. Liu, A. D. McLean, and M. Yoshimine, Phys. Rev. A 5, 1614 (1972).
[35]R. J. LeRoy, University of Waterloo Chemical Physics Research Report No. CP-110 (unpublished).
[36]M. Gerard, T. R. Govers, and R. Marx, Chem. Phys. 30, 75 (1978).
[37]A. Antić-Jovanović, V. Bojović, D. S. Pesić, and S. Weninger, J. Mol. Spectrosc. 75, 197 (1978).
[38]I. Botterud, A. Lofthus, and L. Veseth, Phys. Scr. 8, 218 (1973).
[39]N. Elander, J. Oddershede, and N. H. F. Beebe, Astrophys. J. 216, 165 (1977).
[40]R. N. Zare, A. L. Schmeltekopf, W. J. Harrop, and D. L. Albritton, J. Molec. Spectrosc. 46, 37 (1973).
[41]D. L. Albritton, A. L. Schmeltekopf, and R. N. Zare, an introduction to the least-squares fitting of spectroscopic data, in *Molecular Spectroscopy: Modern Research II*, edited by K. Narahari Rao (Academic, New York, 1976), Chap. 1.
[42]P. W. Atkins, *Quanta, A Handbook of Concepts, Oxford Chemistry Series* (Clarendon, Oxford, 1974), p. 54.
[43]H. Helm, P. C. Cosby, D. L. Huestis, and R. P. Saxon, J. Chem. Phys. (in press).
[44]I. Kovács, *Rotational Structure in the Spectra of Diatomic Molecules* (American-Elsevier, New York, 1979).
[45]J. B. A. Mitchell, Irish Astron. J. 113, 109 (1977).
[46]S. S. Prasad and W. T. Huntress, Jr., Ap. J. Supp. 43, 1 (1980).
[47]K. Kirby, W. Roberge, R. P. Saxon, and B. Liu, Astrophys. J. 239, 855 (1980).